JCTC Journal of Chemical Theory and Computation

Base Flipping in a GCGC Containing DNA Dodecamer: A Comparative Study of the Performance of the Nucleic Acid Force Fields, CHARMM, AMBER, and BMS

U. Deva Priyakumar and Alexander D. MacKerell, Jr.*

Department of Pharmaceutical Sciences, School of Pharmacy, University of Maryland, Baltimore, Maryland 21201

Received August 5, 2005

Abstract: The improving quality of empirical force field parameters along with other methodological improvements and ever increasing computational resources have lead to more reliable computations on biological macromolecules. In the case of oligonucleotides, three force fields, namely CHARMM27, AMBER4.1, and BMS, have been developed and are widely used by the simulation community. Testing of these force fields to date has primarily focused on their treatment of the canonical forms of DNA and RNA. However, many biological functions of oligonucleotides involve significant variation of their structures from the canonical forms. In the present work, the three force fields are evaluated via computation of potentials of mean force (PMF) of the base flipping process in a DNA dodecamer, 5′-GTCAGCGCATGG-3′. Results are compared with available experimental data on the equilibrium between the opened and closed (i.e. Watson−Crick base paired) state of the underlined C and its WC partner G. Quantitative analysis shows CHARMM to be in the best agreement with experiment, closely followed by AMBER with BMS in the poorest agreement. Various components contributing to the change in the free energy such as base pair interactions, stacking interactions, solvation effects, and intrinsic potential energy changes were evaluated and compared. The results indicate that while all three force fields reasonably represent the canonical structures, the balance of forces contributing to their structural and dynamic properties differ significantly.

Introduction

Molecular dynamics simulations play a dominant role in understanding the relationships among structure, energetics, and function of biological macromolecules.[1−3] While these calculations are helpful in explaining various experimental observations, they are indispensable in investigating properties that are otherwise difficult or inaccessible to experiments, including high-energy states sampled during conformational transitions. These attributes include the ability to obtain energetic information on conformational transition and relate that information to structural properties at an atomic level of detail. Accordingly, an important consideration when applying MD simulations to biological macromolecules is the quality of the empirical force field being used to correctly represent the relationship between structure and energetics. The past decade has witnessed tremendous progress in the development of these force fields, thereby enabling more reliable computations on biomolecules in general and nucleic acids in particular.[3−12] Various force fields optimized for nucleic acids are available, including the CHARMM27,[13,14] AMBER4.1,[15,16] and Bristol-Myers-Squibb (BMS)[17] all-atom force fields. To date, tests of these force fields have focused on the canonical structures of DNA and RNA. These tests have indicated that the above force fields satisfactorily treat the canonical structures, although limitations in each of the force fields have been noted.[17−21] In the present paper we extend the tests of these force fields to include a conforma-

* Corresponding author phone: (410)706-7442; fax: (410)706-5017; e-mail: amackere@rx.umaryland.edu. Corresponding author address: 20 Penn Street, Baltimore, MD 21201.

10.1021/ct0501957 CCC: $33.50
Published on Web 11/16/2005

tional transition to a noncanonical conformation of DNA, namely base flipping.

Base flipping is a process by which one of the bases of the DNA is displaced from its base paired state, moving out of the double helix typically leaving its WC-base paring counterpart in its original position.[22−26] Such a process, though energetically unfavorable, is favored during interactions with selected proteins, which assist flipping of the base to perform chemical reactions on the otherwise inaccessible base.[23,25,27−29] Base flipping is also adopted by transcription proteins in order to achieve stable protein−DNA complexes.[22,30] In the absence of a protein, nucleic acids undergo base opening whose dynamics have been extensively studied using NMR imino proton exchange experiments on various sequences.[31−35] These experiments yield base opening rates along with the equilibrium between the open and closed states assuming a two-state model. Taking advantage of these data, a direct comparison of the equilibrium between the open and closed states from potential of mean force (PMF) calculations based on MD simulations has been performed.[36]

The present study focuses on evaluation of the CHARMM-27, AMBER (Parm94), and BMS nucleic acid force fields in modeling base flipping in a DNA dodecamer, 5′-GTCAGCGCATGG-3′. PMF calculations for the flipping of the underlined C and its WC base paired counterpart, G, were performed. Equilibrium constant for the base opening/closing process were calculated using the PMFs generated with all the force fields, and the results were compared with the available experimental data. The results are presented and discussed in the following order: Justification of the current methodology and the adequacy of the length of the simulation are discussed followed by presentation of the free energy profiles corresponding to base flipping computed using the three force fields. This is followed by the comparison of the theoretical and experimental data of the equilibrium between the closed and open states. Finally, various factors that affect the base flipping process such as disruption of base pairing and stacking interactions, solvation effects, and intrinsic energetic properties of the DNA are discussed.

Methods

All calculations were performed using the CHARMM program.[37,38] Three different force fields were employed, CHARMM27,[13,14] AMBER4.1 (PARM94),[16] and Bristol-Myers Squibb (BMS).[17] Initially, coordinates for the DNA in the canonical B-form were generated using QUANTA[39] and overlaid onto a preequilibriated solvent box containing sodium ions. The solvent shell extended approximately 8 Å beyond the DNA along the helical axis and 20 Å perpendicular to the axis. Those solvent molecules or the sodium ions whose non-hydrogen atom were within 1.8 Å of non-hydrogen atoms of the DNA were removed, and then the number of the sodium atoms was adjusted to attain electrical neutrality. The systems were minimized for 500 Adopted-Basis Newton Rapheson (ABNR) steps with harmonic constrains of 2.0 kcal/mol/Å on the non-hydrogen atoms of the DNA followed by a 20 ps molecular dynamics simulation in the NVT ensemble. The CRYSTAL[40] module in CHARMM was used for the periodic boundary conditions, and electrostatic interactions were treated using the Particle Mesh Ewald method.[41] Real space electrostatic and Lennard-Jones cutoffs were 12 Å with a switch smoothing function from 10 to 12 Å for the LJ term. The nonbond list was maintained to 14 Å and heuristically updated. The final configurations from the NVT simulation were subjected to minimization for 500 ABNR steps and then a 500 ps NPT MD simulation without any constraints. The final conformations from the 500 ps simulation were taken for the PMF calculations.

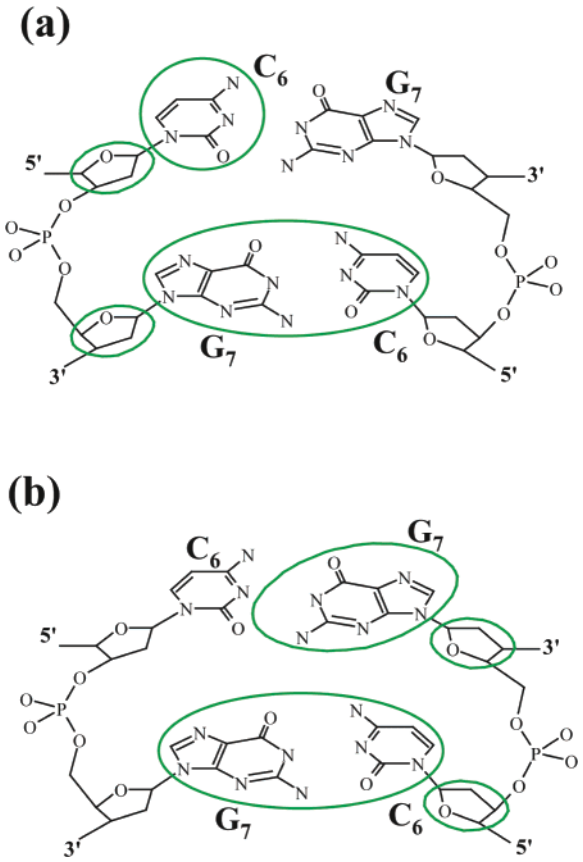

Figure 1. Schematic representation of the center of mass pseudodihedral angle for target C- and G-base flipping (a and b).[36] The dihedral angle formed by the centers of mass of the atoms in the four circles is termed the COM pseudodihedral angle. Values of ∼10° and ∼30° correspond to the WC base paired state in the free energy profiles for C- and G-base flipping, respectively.

Base flipping PMFs were obtained by performing 72 independent MD simulations (i.e. windows) with different pseudodihedral center of mass (COM) restraints (Figure 1) in 5° increments from 0 to 360° from which the probability distributions were obtained for calculation of the free energy surfaces.[36] The COM pseudodihedral angle is defined by the dihedral angle formed by four coordinates defined based on the centers of mass of four sets of atoms: (a) the GC base pair 3′ to the flipping base, (b) the sugar attached to the adjacent base 3′ to the flipping base, (c) the sugar attached to the flipping base, and (d) the flipping base (Figure 1). Initial conformations corresponding to the 72 flipped states for the target C and G bases being flipped were generated as previously described.[36] Briefly, an initial structure corresponding to the first window ($x = 0°$) was obtained using a

0.5 ps simulation with a harmonic potential (force constant = 10 000 kcal/mol/rad^2) on the COM pseudodihedral angle. For the remaining windows, the flipped conformers along both grooves were obtained by performing a series of 0.5 ps MD simulations in the presence of the harmonic potential incremented by ±5° from the final structure from the previous window. This was repeated via both grooves out to 180° yielding the 72 starting structures. The resulting coordinates corresponding to the 72 different flipped conformations of the DNA were then overlaid onto a water sphere of radius 35 Å. The solvent molecules whose non-hydrogen atom was within 1.8 Å of any non-hydrogen atom of the oligonucleotide were deleted, and the number of sodium ions was adjusted to attain electrical neutrality. The resulting systems were then subjected to a 500 step steepest descent minimization, and equilibration of each window was done for 60 ps followed by a 160 ps production run. Nonbond interactions were treated via atom based truncation with the nonbonded lists updated heuristically with a list cutoff of 14 Å, a nonbond cutoff of 12 Å, and the smoothing functions initiated at 10 Å. Electrostatic and LJ interactions were smoothed using the force shift and force switch methods, respectively.[42] An integration time step of 2 fs, a temperature of 300 K, and SHAKE[43] to constrain the covalent bonds involving hydrogen atoms were used during the NVT simulation applying the Nosé-Hoover temperature coupling scheme.[44] During the minimization, equilibrium, and production runs, the following restraints were imposed: (a) the terminal base pairs of the DNA were harmonically restrained to their initial spatial coordinates using a force constant of 2.0 kcal/mol/Å; (b) water density of the systems was maintained by using the mean field solvent boundary potential included in the miscellaneous mean field potential (MMFP) module in CHARMM;[45] and (c) a harmonic umbrella potential, $w_i(x) = k_i (x - x_i)^2$ (k_i is the force constant, 1000 kcal mol^{-1} rad^{-2}; x is the center of mass (COM) dihedral angle; and x_i is the restrained value of the angle) was used for the COM pseudodihedral angle. The value for the pseudodihedral angle was recorded every time step during the simulation for obtaining the probability distributions; other analyses were performed on time frames recorded every 1 ps of the trajectories. PMFs were obtained using the weighted histogram analysis method (WHAM) procedure that enforces periodicity of the reaction coordinate,[46,47] with a width of 0.5° for the pseudodihedral angle as previously described. Stacking interaction of the flipping base with its neighbors were calculated by considering both electrostatic and van der Waals terms using the INTER command implemented in CHARMM.[48] The neighboring bases immediate to the flipping base and their base pair counterparts in the complementary strand were considered for these calculations using the real space nonbond interaction cutoffs listed above. Calculation of the stacking interactions involved only the specified nucleic acid bases and not the sugar or phosphate groups.

Results and Discussion

Adequacy of the Sampling. Essential for the validity of the theoretical-experimental quantitative comparison is the convergence of the obtained free energy profiles; hence, the adequacy of the length of the 72 simulations comprising the PMF was first verified. For each free energy profile generated, each simulation (i.e. window) was performed for 220 ps, yielding a sum for all 72 simulations defining each PMF of 4.3 ns for the equilibration and 11.5 ns for the production runs. MacKerell and co-workers have performed limited tests on the convergence issues with respect to the length of the simulation and found that 220 ps MD simulation (i.e. 60 ps equilibration plus 160 ps production) for each window is long enough for satisfactory convergence.[49] To further validate the adequacy of the length of the simulations for the three force fields, the PMFs with respect to the length of the simulation were calculated for every 20 ps range from 60 to 220 ps (Figure S1 in the Supporting Information). The free energy profile obtained for the whole 60−220 ps range is also given for comparison. The PMFs overlap after the initial 60−80 ps sampling periods fluctuating around the 60−220 ps surfaces. In addition, the 72 MD simulations that used the CHARMM force field were each extended to 440 ps. The free energy profiles calculated from the 60−220 ps, 220−440 ps, and 60−440 ps windows are given in Figure 2. Comparison of the PMFs from these sampling ranges shows only minor differences with respect to the increase in sampling. While not absolute proof, behavior of the PMFs strongly suggests that they are adequately converged at 220 ps to allow for quantitative analysis and detailed structural and energetic analysis of the flipping profiles.

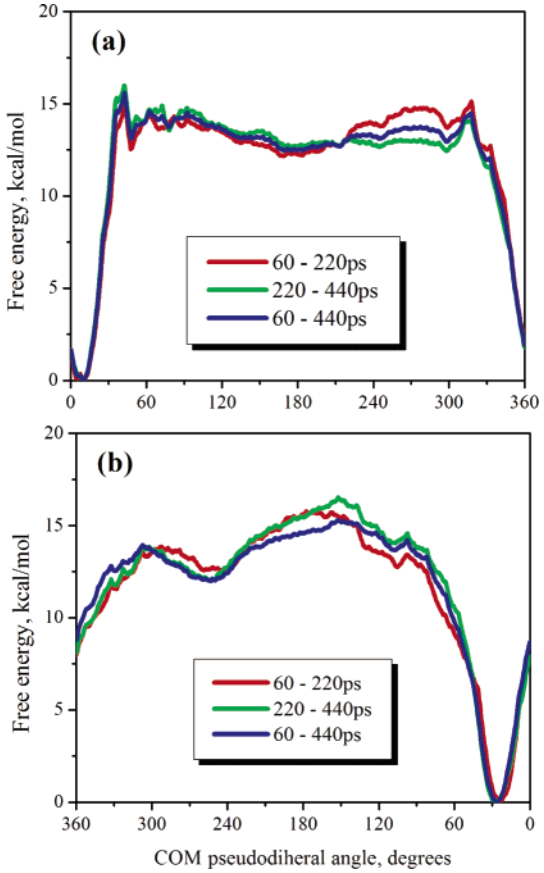

Figure 2. PMFs obtained for the C- (a) and G-base (b) flipping using the 60−220, 220−440, and 60−440 ps windows of the MD simulations using the CHARMM force field.

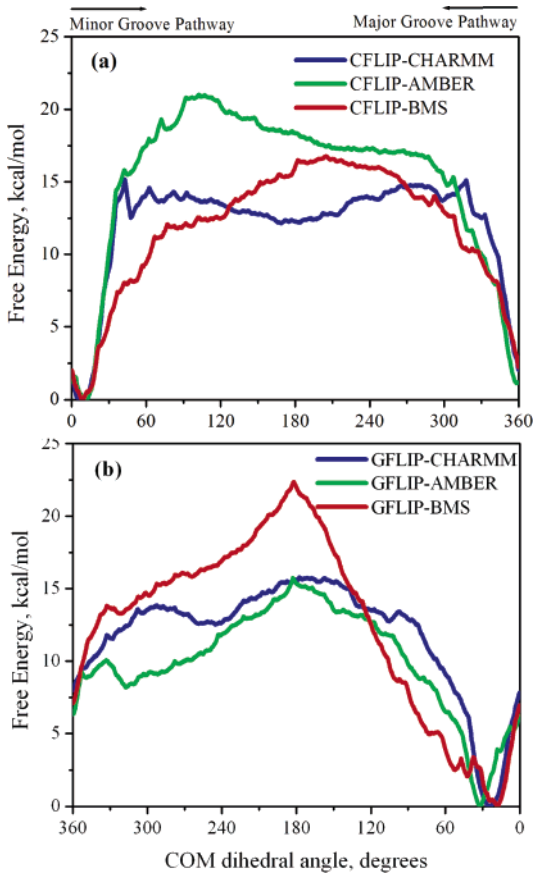

Figure 3. Free energy profiles obtained using CHARMM (blue), AMBER (green), and BMS (red) force fields as a function of the COM pseudodihedral angle (Figure 1) for C-base flipping (a) and G-base flipping (b). The free energies were calculated using the 60−220 ps windows of the MD simulations.

Free Energy Profiles. The PMFs calculated for the target C- and G-base flipping are depicted in Figure 3 (parts (a) and (b), respectively) for the CHARMM, AMBER, and BMS force fields. Inspection of these figures indicates that the free energy profiles predicted using the three force fields are quite different both qualitatively and quantitatively. In the case of C-flipping, the WC base paired state at a pseudodihedral angle of ∼10° is predicted to be the minimum energy structure by all the three force fields (11, 11, and 9° by CHARMM, AMBER, and BMS, respectively). However, the shapes of the profiles and the barrier heights for base flipping give rise to three different scenarios. The free energy profiles obtained using CHARMM and AMBER indicate that the energy increases sharply when the target C base flips out of DNA duplex from both the major and minor grooves, whereas with BMS, the increase in energy is gradual especially along the minor groove pathway. The CHARMM PMF exhibits a broad, shallow minimum of approximately 2.5 kcal/mol in the range of 60−320° for the C-base flipped state with an energy of approximately 12 kcal/mol above the global minimum. The energy barrier for flipping from the minor and major grooves is around 16 kcal/mol. This is consistent with the previous computational and experimental studies, which predict that the base flipping via both the minor and major grooves is feasible.[36,50−54] In contrast to CHARMM, the other two force fields do not have a minimum for the flipped out state. The flipping profile obtained with AMBER indicates that the minor groove pathway is energetically more expensive by about 4 kcal/mol than the major groove pathway. This is consistent with the conventional wisdom that for the base to move out via the minor groove, it has to overcome steric effects from the close lying backbone compared to the major groove side. BMS, on the other hand, predicts a more gradual increase of energy via the minor groove and a sharp increase via the major groove, which indicates that the former pathway is slightly preferred over the other. With both AMBER and BMS single distinct maxima occur in the PMF at ∼100 and ∼200°, respectively. Irrespective of the force field employed, the results indicate that the change in free energy among the various flipped states (COM pseudodihedral angle range of ∼60 to 300°) is not drastic. This implies that once the base flips out, it is expected to sample a wide range of conformations.

Results for G-flipping for the 3 force fields are presented in Figure 3(b). The pseudodihedral angle at which the WC base pairing occurs for G-flipping is different from that in the C-flipping profiles based on the definitions of the flipping pseudodihedral angle as is the direction of the rotation corresponding to minor versus major groove flipping.[36] Accordingly, the *x*-axis is reversed to allow for visualization of the minor and major flipping pathways to coincide for C- and G-flipping. The free energy profiles calculated using the three force fields show COM pseudodihedral angles at which WC base paired states occur slightly deviate from each other (25° for CHARMM, 32° for AMBER, and 18° for BMS). This may be due to slight deviations in relative orientations of the sugar and the adjacent GC base pairs, which are used to define the pseudodihedral angle. Qualitatively, the change in the free energies with respect to the pseudodihedral angle computed by CHARMM and AMBER are similar, especially via the major groove pathway. Both AMBER and BMS have distinct maxima at ∼170°, with BMS lacking any significant local minima for the flipped state; such states are seen with CHARMM and AMBER at approximately 240 and 310°, respectively. However, these minima are shallow, being ∼2 kcal/mol deep. Overall, it is evident that while all three force fields show the distinct minima associated with the WC base paired states, there are significant qualitative differences between the models.

Imino proton exchange studies on a GCGC sequence indicate the presence of local minima for the fully flipped state which lies about 9 kcal/mol above the WC base paired state.[32] In the free energy profiles for C-flipping with CHARMM and G-flipping for both CHARMM and AMBER local minima are present, though these minima are shallow. Experimental studies have shown that the lifetime for the WC base paired state is in the order of milliseconds, and the proposed base open state corresponds to a metastable state with a lifetime in the nanosecond range.[33,55,56] Based on the difference of approximately 10^6 between the lifetimes of the WC and flipped minima, the difference between the barriers corresponding to base closing and opening processes is calculated to be about 14 kcal/mol according to the

transition state theory and assuming that the preexponential contributions are identical for the two processes. In the present study, CHARMM predicts a shallow minimum for the flipped out state for both C- and G-flipping. The differences in the barrier corresponding to base opening and closing calculated using the CHARMM free energy profiles are 12.1 and 11.8 kcal/mol for C- and G-flipping, respectively, which is consistent with the experimental results.

Comparison of Experimental and Calculated Equilibria between the Open and Closed States. Base flipping leads to exposure of the imino proton of the bases, which are otherwise hidden in the DNA duplex, to the solvent environment. Upon exposure, the imino protons from G-H1 or T(U)-H3 undergo exchange with the solvent. This process has been extensively used to measure the opening and closing rates of the bases and the equilibrium between the open and closed states in nucleic acids.[31−33,57,58] Quantitative analysis of these experiments is based on a two-state model where the equilibrium between the two states is studied within the assumption that the imino protons in the closed state are not accessible for exchange. Experimentally, it has been observed that the base pairing and opening process occurs on the millisecond time scale with the equilibrium between the open and closed states typically in the range of 10^{-7}. In particular, experiments on DNA containing a central GCGC sequence have yielded an equilibrium constant of 3.3×10^{-7}.[32] This value may be used for quantitative evaluation of the present PMFs, as previously performed.[36] It should be noted that estimates of the free energy of opening have been made based on the measured opening rates. However, exact calculation of the activation free energy of opening requires knowledge of the preexponential term in transition state theory.[59,60]

To calculate equilibrium constants, the 72 windows have to be assigned to open or closed states, following which summation over the probabilities for the two states allows for calculation of the equilibrium constants. Base open states are defined as those conformations whose imino proton is accessible for exchange with solvent, though they may partly be base paired. To identify the windows that comprise the open state, the solvent accessible surface area[61] of the N1 and H1 atoms of the guanine base was calculated using a probe radius of 1.4 Å with an accuracy of 0.01 Å, with those windows having an accessibility greater than zero assigned as being open. To obtain the probabilities of each state, the PMFs were converted to probability distributions based on a Boltzmann distribution. The mean solvent accessibilities and the probabilities as a function of the COM pseudodihedral angles for the C- and G-flipping obtained using CHARMM, AMBER, and BMS are depicted in Figure 4. Expectedly, the solvent accessibility of the base open and closed states differ significantly in the case of C- versus G-flipping due to differential exposure of the G(H1) imino proton to the environment. For C-flipping (Figure 4a−c), the G base stays in the duplex and hence the solvent accessibility difference is not large; however, the imino proton is accessible for exchange when the C-base flips out as reflected in the variation of the solvent accessibilities as a function of COM dihedral angle.Based on the solvent accessibilities, the conformers were grouped into open and closed states based on the COM dihedral angle as listed in Table 1. The equilibrium constants calculated by integrating the unbiased probability distributions over the open and closed states along with the experimental data are also given in Table 1. The equilibrium constants for the C- and G-base opening have to be summed as the experimental data corresponds to both C- or G-base opening. From the results it is evident that CHARMM yields the best agreement with experiment, followed by AMBER with BMS in relatively poor agreement. These observations hold when variations in the windows selected for calculation of the PMF are tested, as shown in Tables S1−S3 of the Supporting Information. With both AMBER and BMS the calculated equilibrium constants are larger than the experimental values. This indicates that the open states are more favored in the force fields as compared to the experimental regimen. To better understand this behavior as well as compare how the various components of the force fields contribute to the calculated equilibria and PMFs, analysis of different structural and energetic terms as a function of the COM pseudodihedral was undertaken.

Potential Energy Contributions to the Base Flipping Free Energy Profiles. To better understand the atomistic contributions to the flipping PMFs, changes in potential energies as a function of the flipping free energy surfaces were obtained. Energetic contributions analyzed included the interaction energy between the flipping base and its WC base pairing partner, stacking interactions of the flipping base with its neighbors, interaction of the flipping base with the remainder of the DNA, interaction energies with the solvent and intrinsic energetics of the DNA itself. The initial analysis involved looking at changes in the interaction energy of the flipping base with the remainder of the DNA and with the solvent environment. Presented in Table 2 are the energy differences for the two terms between the WC states and the flipped states, where the values for the flipped states are averages over windows 180−210°, inclusive. Table S4 of the Supporting Information includes the average values for the two states, and Figure S2 shows the changes as a function of the extent of flipping. As may be seen, upon flipping the interaction energy of the base with the remainder of the DNA become less favorable due to the expected decrease in the favorable interactions between the flipping base and the DNA, with that loss of energy being similar for CHARMM and AMBER, while the value with BMS is larger. Opposing the loss of base−DNA interactions are gains in the energy of solvation of the tribase; in this case the CHARMM and AMBER values are significantly more favorable than that observed with BMS. Analysis of the magnitudes of the flipping base−DNA and solvation terms shows them to be larger than the free energy differences of approximately 15 kcal/mol for both C- and G-flipping (Figure 3). Thus, the present results indicate that the free energy of flipping is associated with large interactions of the flipping base with the remaining DNA and with the solvent environment, with those contributions acting to compensate for each other, yielding a smaller free energy difference than those components themselves. In addition, it is clear that differences in these terms exist between the force fields; additional

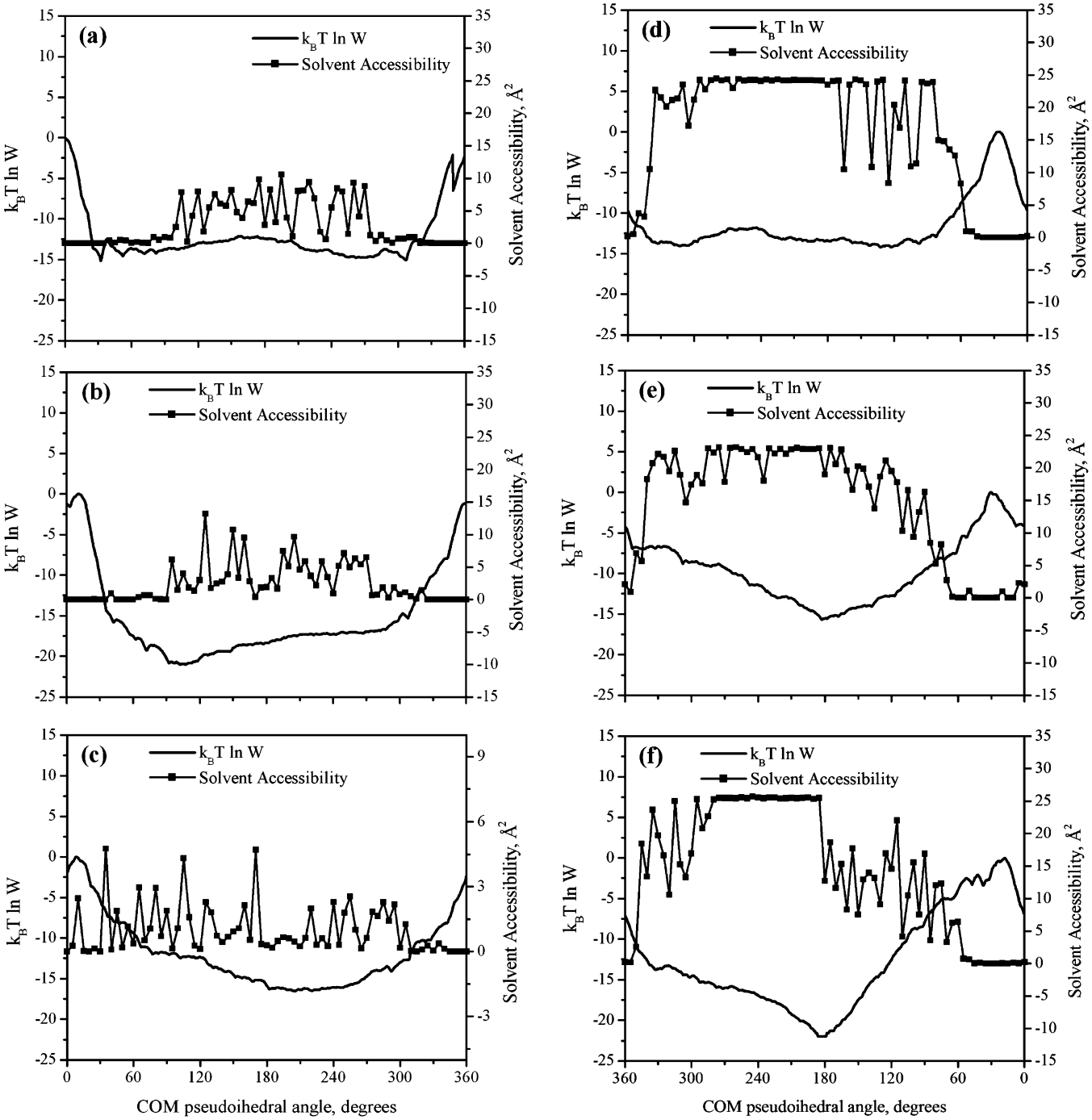

Figure 4. Solvent accessibilities (filled circles) of the imino proton of the orphan G averaged over the final 160 ps of the MD simulations and the Boltzmann weighted logarithm of the unbiased probability densities (solid line) obtained for C- (a, b, c) and G-base flipping (d, e, f) using CHARMM (a and d), AMBER (b and e), and BMS (c and f).

analysis will focus on obtaining a more detailed understanding of the contributions to these differences.

Base Pairing Interactions and Watson−Crick Hydrogen-Bonding Distances. The most obvious consequence to the DNA when one of the bases flips is the disruption of the hydrogen bonds formed in the native WC base paired state. The correlation of the N3(G)−N1(C) distance and the GC base pair interaction energy averaged over the final 160 ps with respect to the COM dihedral angle are given in Figure 5; the PMFs obtained are also depicted for comparison. Notable is the significant difference in the total GC interaction energy for the three force fields. The base pair interaction energies are offset to the value corresponding to the WC base paired state. The average GC interaction energies at the WC base paired states are computed to be 21.9, 26.3, and 26.2 kcal/mol using CHARMM, AMBER and BMS, respectively. These values are similar to GC base pair interaction energies published in the literature,[13,17,62,63] though differences exist due to subtle changes in the geometry of the DNA and methodological differences. Notably, both AMBER and BMS force fields significantly overestimate the interaction energies as judged by both quantum mechanical and experimental data.[13,63,64]

Table 1: Equilibrium Constants for the Equilibrium between the Base Open and Closed States Calculated Using CHARMM, AMBER, and BMS along with the Experimental Value[a]

method	C-flip	G-flip	total
CHARMM			
open states	75−320°	55−345°	
equilibrium constant	1.1×10^{-8}	3.6×10^{-7}	3.8×10^{-7}
AMBER			
open states	60−325°	65−355°	
equilibrium constant	4.6×10^{-9}	7.1×10^{-6}	7.1×10^{-6}
BMS			
open states	60−300°	70−350°	
equilibrium constant	6.1×10^{-8}	2.1×10^{-4}	2.1×10^{-4}
exptl equilibrium constant			3.3×10^{-7}

[a] Included are the ranges of the COM dihedral angles of the conformers considered as base open states used for calculation of the equilibrium constants. Open states defined based on the COM pseudodihedral angles. Closed states are all states not defined as open states.

Table 2: Differences in Interaction Energies between the WC and Fully Flipped States for the Flipping Base with the Remainder of the DNA and for the Flipping Base, the Central Tribase (GCG), and the Backbone of the Tribase with the Solvent and Their Solvent Accessible Surface Areas Obtained using the CHARMM, AMBER, and BMS Force Fields[a]

	CHARMM	AMBER	BMS
base to DNA interaction energy			
C-flip	37.1	35.3	51.0
G-flip	51.4	55.9	65.7
base to solvent interaction energy			
C-flip	−23.7	−24.6	−37.7
G-flip	−39.2	−41.0	−52.9
backbone to solvent interaction energy			
C-flip	−23.4	−18.3	0.1
G-flip	−25.8	0.5	−3.1
tribase to solvent interaction energy			
C-flip	−80.8	−79.2	−47.8
G-flip	−95.3	−90.2	−48.1
base solvent accessible surface area			
C-flip	17.0	19.2	5.7
G-flip	21.6	20.8	7.0
backbone solvent accessible surface area			
C-flip	−63.5	−14.9	−24.5
G-flip	−31.1	36.4	−79.1
tribase solvent accessible surface area			
C-flip	245.2	276.9	82.2
G-flip	247.4	239.5	57.9

[a] Interaction energies are given in kcal/mol and solvent accessibilities in Å^2. Individual energies along with error estimates from which the differences in this table were calculated are presented in Table S4 of the Supporting Information.

Expectedly, the N1−N3 distance increases and the GC base pairing interaction energy decreases in all the cases when the COM dihedral does not correspond to the WC base paired state. The change in the N1−N3 distance correlates well with the base pair interaction energies and also with the free energy changes. For C-flipping via the minor groove, the base pairing interaction is maintained up to approximately 40° (35° in case of BMS) beyond the WC base paired state with a drastic decrease in the interaction energy at this angle when going further from the WC base paired state. Interestingly, the barrier for C-flipping via the minor groove occurs at the position that the N1−N3 distance shows a marked increase with CHARMM and AMBER. Whereas from the major groove CHARMM predicts a gradual decrease in the interaction energy (i.e., becomes less favorable) and an increase in the N1−N3 distance for the pseudodiheral angle from 10 though 0° down to 315°. AMBER and BMS predict a similar change in these terms but with sudden jumps between; this behavior may contribute to the more gradual increase in the free energy profiles observed in that region for those force fields.

In the case of G-flipping (Figure 5d−f), the change in the base pair interaction as a function of the COM dihedral angle is similar in the sense that the decrease is sudden from the minor groove and gradual from the major groove. Interestingly, base paring is well maintained out to 65° in the case of AMBER as reflected in both the N1−N3 distance and interaction energy; this may be due to the overestimation of base pairing energies, which makes the orphan C base move with the flipping G base. In general, during G-flipping the orphan C base is pushed out of the DNA duplex and moves with the flipping G base along both grooves. In contrast, C-flipping requires the orphan G base to be pushed out only via the minor groove. This can be explained based on the size of the flipping base and the steric constraint via the minor groove pathway.

Stacking Interactions. Inter- and intrastrand stacking interactions of a given base with its neighbors contribute to the overall stability of the oligonucleotides.[48,65−69] During base flipping, the π-stacking stabilizing interaction of the flipping base with its neighbors is expected to change vastly; hence, this could be one of the major factors influencing the base flipping process. The average stacking interactions of the flipping C and G bases with their neighbors are depicted in Figure 5 as a function of the pseudodihedral angle. The stacking interactions of the orphan base with its neighbors were also calculated; however, we observed no appreciable variation with respect to the pseudodihedral angle. In the case of C-flipping, the stacking interactions do not start diminishing significantly via the minor groove as flipping initially proceeds from the WC base paired state (up to 75, 90, and 65° using CHARMM, AMBER, and BMS, respectively). Unexpectedly, the interaction is considerably more favorable in this region compared to that at the base paired state. This is due to the method used to calculate base stacking, such that the formation of hydrogen bonds between the flipping base with the neighboring bases that occur as the plane of the flipping base no longer stays parallel to those of the other bases, contribute to the stacking energy. Examples of such interactions with the CHARMM force field are shown in Figure 6. With AMBER this effect is significant, being <-10 kcal/mol as compared to that observed in the WC base paired state. Interestingly, this occurs despite the C stacking energy being the least favorable in AMBER as compared to CHARMM and BMS. With all three force fields the favorable stacking energy is maintained during minor groove flipping to larger pseudodihedral angles

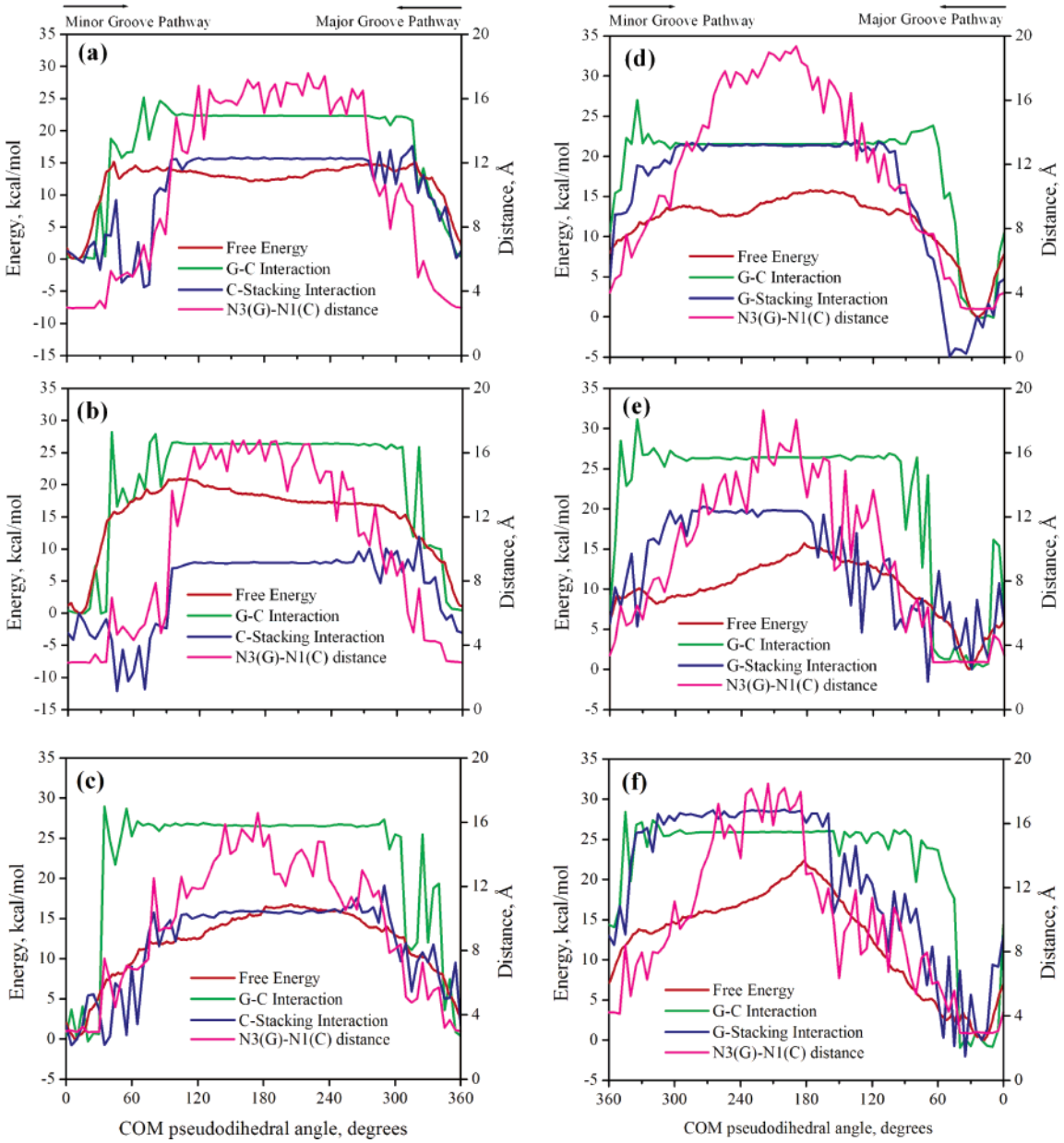

Figure 5. The change in the free energy (red), average N3(G)−N1(C) distance (purple), average G−C base pairing interaction energy (green), and average stacking interaction energy (blue) for C- (a, b, c) and G-base flipping (d, e, f) as a function of the COM pseudodihedral angle calculated using CHARMM (a and d), AMBER (b and e), and BMS (c and f). Base pairing interaction energies and stacking interactions were offset by the corresponding values at the WC base paired state. Stacking interaction energies were calculated with the neighboring bases of the same strand as the flipping base.

than the WC interaction energy. This is, in part, due to interactions of the flipping C base with the adjacent bases in the minor groove. These types of interactions have previously been reported and have been suggested to represent a mode for the effect of sequence on base flipping.[36] The fact that this phenomenon is observed in all three force fields indicates that it is not force field specific. With major groove C-flipping, the change in the stacking interaction energy is gradual, similar to that observed in the base pairing energies. The differences between the energetic changes during minor versus major groove flipping have previously been attributed to the need for the partner base to be "pushed" out of the way during minor groove flipping, which during major groove flipping gradually pulls away from the partner base.[36] Accordingly, the gradual loss of stacking energy is due to this type of motion during major groove flipping.

Stacking interactions during G-flipping show somewhat contrasting behavior to C-flipping (Figure 5). The AMBER and CHARMM stacking interaction energies are similar, while that with BMS is significantly more favorable. Here, the maintenance of stacking interactions while WC interactions are lost occurs via the major groove, with CHARMM showing a gain in stacking interactions in the vicinity of 50°. Consistent with the explanation for minor groove C-flipping this is due to the need for the flipping G base to push the partner C base out of its path during flipping. Again, interactions between the flipping base and the atoms in the grooves of the surrounding bases are observed.

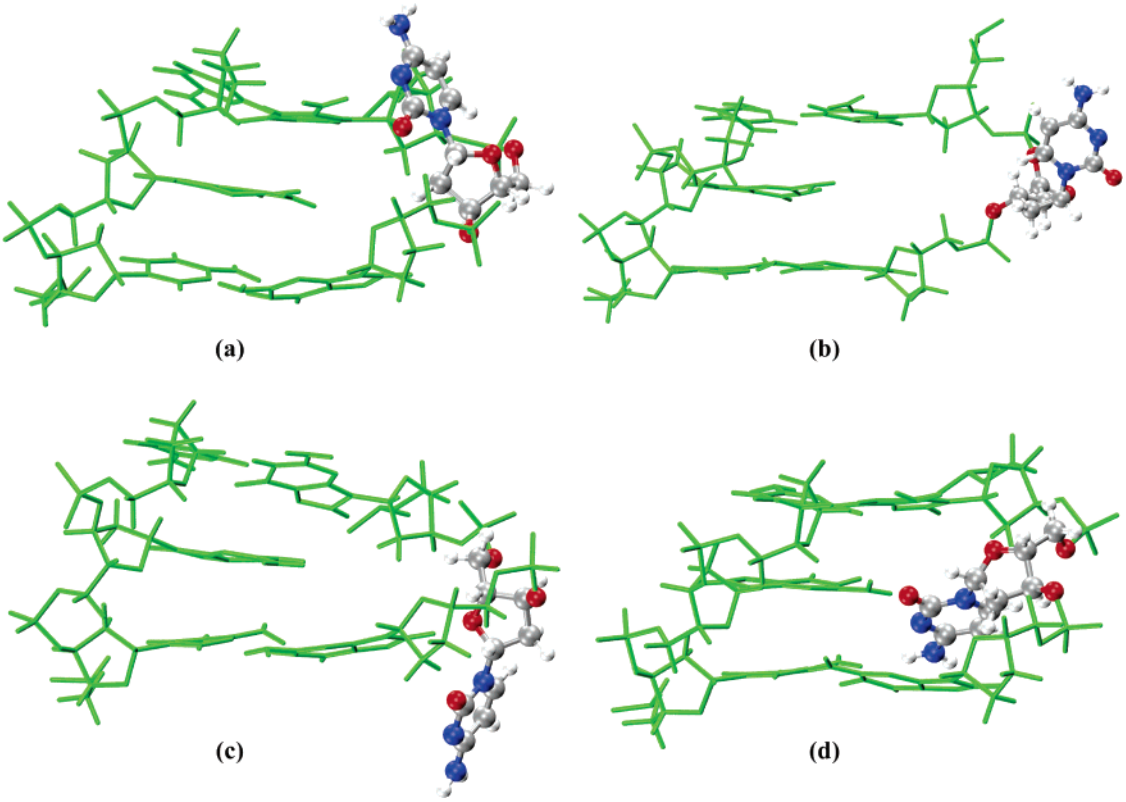

Figure 6. Representative structural snapshots from the MD simulations for C-flipping using the CHARMM force field for COM pseudodihedral angles of 80° (a), 115° (b), 280° (c), and 335° (d) showing the flipping base having favorable interactions with the adjacent bases or the backbone. Only the central tribase (GCG) is shown for clarity; the flipping base along with the sugar to which it is connected is shown in ball-and-stick representation.

Quantifying the accuracy of the force fields in their treatment of stacking is difficult. Previous comparisons of AMBER and CHARMM force fields with QM data show reasonable agreement with both models, with AMBER being in better agreement while CHARMM overestimates the interaction energies.[70] However, the quality of the QM data, which used the MP2/6-31G(d′) level of theory, where d′ indicates the use of a smaller exponent on the polarization function than in the normal basis set, is questionable. While the ordering of different stacking pairs and orientations may be reasonable from this level of theory due to the role of electrostatic interactions in that ordering, the absolute values may be less accurate due to limitations in that level of theory as well as QM methods in general in treating dispersion type interactions that dominate the total stacking interaction energy.[70−72] QM calculations with explicit consideration of electron correlation such as CCSD(T) accompanied with large basis sets are expected to provide more reliable data on the stacking interactions. However, state of art computational resources limit such calculations. In addition, the lack of a well-defined minima for these stacking complexes is another limitation.[48,71] Alternatively, is the validation of the stacking interactions via the calculation of experimental heats of sublimation, ΔH_{sub}, of base crystals. Such calculations have been performed for uracil and 9-methyladenine using the CHARMM force field,[13] showing good agreement with experimental data. Assuming that the in plane hydrogen bonding is being accurately treated by the CHARMM force field, as evidenced by the reproduction of experimental and QM data, the ability of the force field to reproduce the experimental ΔH_{sub} is a strong indication of its ability to accurately treat stacking. While the calculations with CHARMM have not been performed directly on the G and C bases, due to the absence of experimental data, its ability to reproduce the available experimental data suggests the model to be reasonably accurate with respect to the experimental regimen.

Solvent Contributions. Solvation effects have a strong impact on the properties of DNA, with one of the best examples being the change from the canonical B to A form of DNA as a function of decreasing water activity.[73] In the case of base flipping the movement of the base from the central region of the DNA duplex out of the helix leads to an increase in the exposure of the base to the aqueous environment. Solvation effects may be assessed by calculating solute−solvent interactions to assess the enthalpic contribution and by solvent accessible surface area (SASA), which accounts for the entropic contributions.[61] The flipping base is the one that experiences the most diverse solvation effects during the base flipping event. Also, the backbone of the DNA vicinal to the flipping base undergoes major conformational change and experiences varied exposure to the surroundings. Accordingly, change in the solvation energies and SASA of the flipping base and the backbone of the central tribase as a function of base flipping were analyzed. Solvation energy and SASA differences between the WC base paired and the fully flipped states are given in Table 2, with the average values for the individual states in

the Supporting Information Table S4. The solvation effects calculated undergo high fluctuations as a function of the pseudodihedral angle, hence, for the flipped state the means were obtained over windows, $x = 180-210°$. The interaction energies with solvent and SASA for all the windows as of function of the pseudodihedral are provided in the Supporting Information (Figures S3−S8). Expectedly, the solvation energies typically become more favorable, and the solvent accessibilities increase when the base flips out of the DNA duplex.

For the base alone, the change in the solvation energies of the C base in flipped DNA is predicted to be less favorable than that of the G base by all three force fields, consistent with the larger size and number of polar moieties on the G base. The differences in the solvation energies for the bases are similar with CHARMM and AMBER, while the BMS values are more favorable, as discussed above. Interestingly, while the change in SASA for the flipping bases are similar for CHARMM and AMBER (∼20 Å^2), they are significantly smaller for BMS, even though the solvation energies are significantly more favorable with the latter. This indicates that the base in BMS interacts more favorably with the solvent as compared to CHARMM and AMBER, while the smaller increase in SASA is due to enhanced interactions of the flipping base with the remainder of the DNA in BMS. Visual inspection of the final structures from the $x = 180°$ windows confirms this model (not shown).

Solvation analysis of the backbone of the flipping base shows relatively small changes upon flipping when considering the magnitude of the solvation energies and SASA values in the WC states (∼500 kcal/mol and ∼650 Å^2, respectively, Table S4, Supporting Information). In some cases the changes are slightly favorable, with the largest being −26 kcal/mol, with others close to zero. For the SASA, interestingly, in many cases there is a decrease in the accessibility in the flipped state. This appears to be due to the interactions of the flipping base with the local backbone atoms. Overall, these results indicate that changes in the solvation of the backbone are not significantly impacting the flipping PMFs.

Changes in solvation of the entire central tribase surrounding the flipping region, which includes both strands, were analyzed as changes would include contributions from the orphan bases and of the bases adjacent to the flipping base. For the tribase, in all cases the energies of solvation become more favorable in the flipped state, while the SASAs were larger. With CHARMM and AMBER, both the energy and SASA differences were similar for the two force fields as well as for C- versus G-flipping. However, with BMS, the magnitudes of the changes in both the energies of solvation and the accessibilities were smaller than with CHARMM and AMBER, though the direction of the change was the same.

Overall, the solvation results indicate only subtle differences between the three force fields with respect to flipping. Considering the base alone, BMS has more favorable solvation energies in the flipped states as compared to CHARMM and AMBER. This more favorable solvation would favor the flipped state, thereby contributing to the significantly larger equilibrium constant the open versus closed states for BMS (Table 1). However, analysis of the solvation of the central tribase shows CHARMM and AMBER to become more favorably solvated in the flipped states as compared to BMS. Thus, the present analysis does not allow for clear conclusions on the role of solvation on the calculated PMFs for the differenct force fields to be obtained.

Table 3: Differences in the Average Intrinsic Potential Energies between the WC and Fully Flipped States for Selected Regions of the DNA Using the CHARMM, AMBER, and BMS Force Fields[a]

	CHARMM	AMBER	BMS
	C-Flip		
tribase	54.7	54.3	38.9
backbone	12.6	7.7	−0.3
six bases	45.5	44.3	19.9
sugar	9.4	8.6	−1.5
phosphate	−0.3	−1.2	−0.8
flipping base	0.7	0.6	1.0
	G-Flip		
tribase	59.4	48.6	25.3
backbone	8.2	2.8	−0.9
six bases	44.9	45.2	37.0
sugar	8.4	2.0	−1.5
phosphate	0.4	−0.4	0.3
flipping base	0.4	−0.1	0.5

[a] All values are given in kcal/mol. Regions of the DNA include the central tribase and the corresponding backbone, six bases, sugar moieties, phosphate groups, and the flipping base. Individual energies along with error estimates from which the differences in this table were calculated are presented in Table S5 of the Supporting Information.

Intrinsic Potential Energy. Variation of the intrinsic potential energy of the DNA along the flipping pathway might be a factor affecting the free energy profiles. The difference of the intrinsic potential energies (i.e. internal molecular mechanical energy of the selected regions, including nonbond contributions) between the WC base paired and the flipped states obtained using the three force fields are given in Table 3. The values for the flipped states were taken as the average value of the windows with $x = 180-210°$. The relative values of the intrinsic potential energies with respect to the WC base paired state are given in Figure 7. Inspection of the figure quickly reveals that BMS yields the smallest increases in the intrinsic energies upon flipping, with the contribution in some cases being favorable. The potential energies of the phosphate groups and the flipping base do not vary much as predicted by all the three force fields. The increase in energy of the tribase, backbone, bases, and the sugar when the base flips out of the DNA duplex is quite substantial and are similar for CHARMM and AMBER. This increase in the energy due to the drastic conformational change seems to be significantly underestimated by BMS. It is interesting to note that the underestimation of the energies mainly corresponds to the neighboring bases of the target base as evidenced by the tribase and six bases results, and this is associated, in part, with the loss of WC and

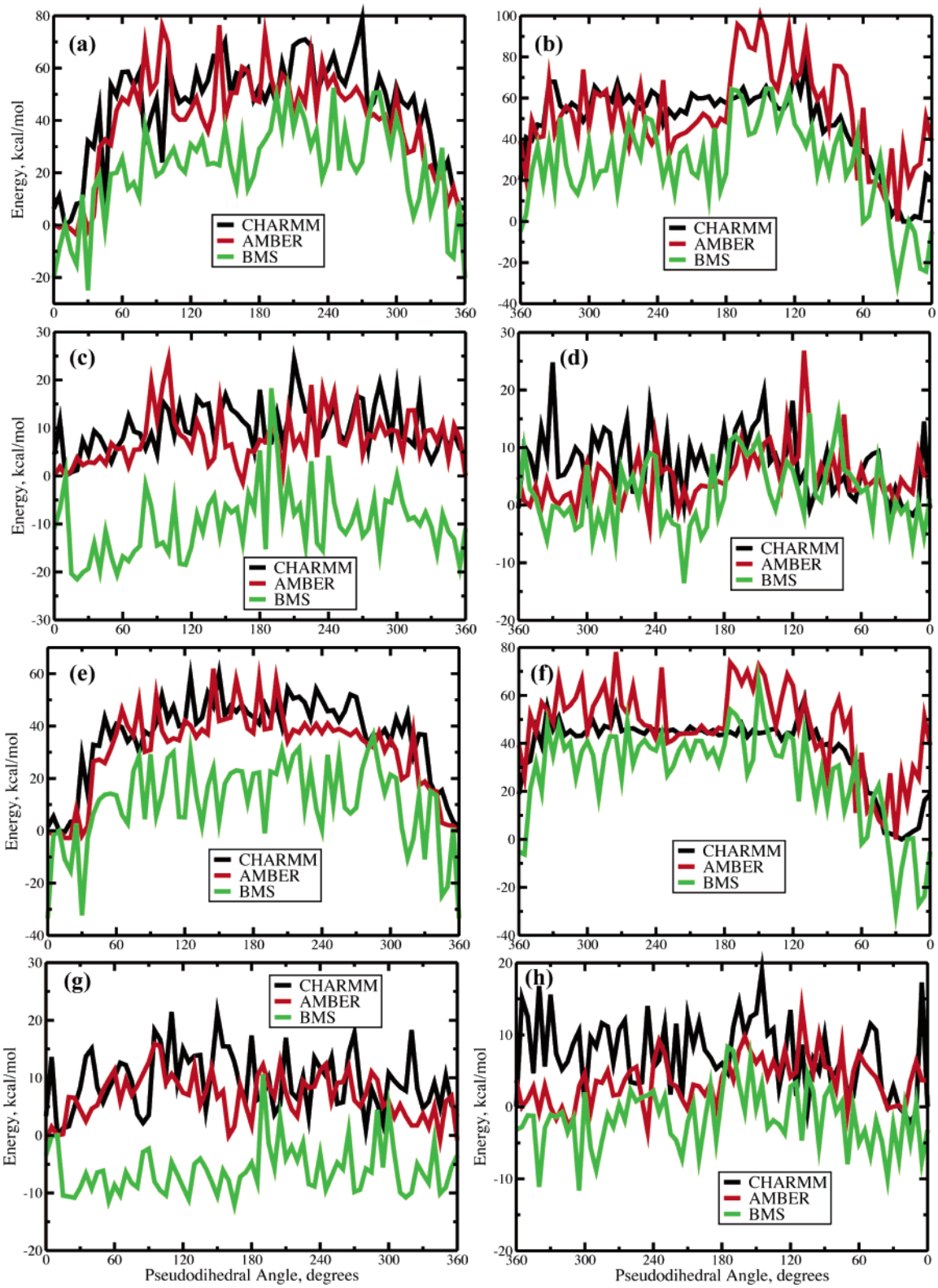

Figure 7. The change in the intrinsic potential energies of central tribase (a and b), backbone of the tribase (c and d), the six bases of the central tribase (e and f), and the sugar moieties of the tribase (g and h) obtained using CHARMM (black), AMBER (red), and BMS (green) corresponding to C-flipping (a, c, e, and g) and G-flipping (b, d, f, and h). The values are offset to those obtained for the WC base paired state.

stacking interactions, as discussed above. Thus, it appears that the intrinsic energetic contributions of the BMS force field leads to the preference of that model for the open state as predicted by the equilibrium constants (Table 1).

Conclusions

The present study reports a comparative assessment of the performance of three popular force fields for nucleic acids, CHARMM, AMBER, and BMS, to reproduce experimental

data from NMR imino proton exchange on the equilibrium between the base open and closed states associated with base flipping from DNA. Free energy profiles, or PMFs, were generated based on the umbrella sampling approach using a COM pseudodihedral restraint as the reaction coordinate. Convergence of the PMFs was critically analyzed; the results indicate that the amount of sampling via the 220 ps of sampling in each window of the PMF via MD simulations is satisfactory, and the conclusions arrived at from the present results are unlikely to change when additional sampling is performed. Comparison of the equilibrium constants between the open and closed states with the experimental data show the CHARMM27 force field to be in the best agreement, closely followed by AMBER with BMS being in significant disagreement. The tendency for both AMBER and BMS is to favor the open state. In addition, CHARMM is consistent with the experimental observation that the base flipped state corresponds to a metastable state lying around 12 kcal/mol above the WC base paired state. However, it should be emphasized that the present results are limited to a single base pair in a single sequence, such that the generality of the present observations requires additional studies.

Qualitatively, the free energy profiles calculated using the three force fields differ significantly with respect to the shape of the surfaces including barrier heights and the presence and depth of stable minima associated with the flipped states. Various components, namely the base pairing and stacking interaction energies and solvation energies, assumed to contribute to the energetics of base flipping, were assessed and shown to correlate with the observed free energy change. The base pair interaction energies for WC GC basepair calculated using the AMBER and BMS force fields are more favorable as compared to CHARMM, with the present values from AMBER and BMS being in disagreement with QM and experimental data. With base stacking significant variations between the force fields are present, though it is currently difficult to evaluate the accuracy of the force fields based on QM data. Changes in solvation energies of the flipping base also differ significantly between the three force fields with CHARMM and AMBER being more similar, while BMS shows more favorable solvation of the flipping base. However, the change in solvation of the central tribase is less favorable with BMS than with AMBER and CHARMM, making it difficult to draw conclusions concerning the solvation contributions to the free energy profiles. Finally, analysis of the intrinsic potential energies of the DNA as a function of flipping indicate systematic differences; CHARMM and AMBER are similar and unfavorable for the flipped states, while those terms with BMS are significantly less unfavorable and, in some cases, slightly favorable for the flipped state. These results indicate that the favoring of the open state by BMS is dominated by intrinsic energetic contributions.

Overall, the results speak to the quality of both CHARMM and AMBER in modeling the structural distortion of DNA associated with base flipping. On the other hand, BMS favors the more open state, although previous studies have shown this force field to model canonical crystal structures of B-form DNA.[7,9,10] However, the individual contributions from the different force fields to the flipping PMFs in some cases vary significantly. Such differences indicate that the behavior of the force fields are based, to some extent, on different relative contributions for different parts of the model and, importantly, emphasize that such force field effects must be taken into account when interpreting results from MD simulations.

Acknowledgment. We acknowledge NIH Grant GM51-501 for financial support and the Pittsburgh Supercomputing Center for computational support. We express appreciation to Dr. Irina Russu for helpful discussions.

Supporting Information Available: Figures depicting the free energy profiles calculated using various windows, target base−DNA interaction, solute−solvent interaction, and solvent accessibilities and tables presenting the equilibrium constants calculated using various ranges of windows, and solvation energies, solvent accessible surface area, and intrinsic potential energies of the WC base paired and flipped states. This material is available free of charge via the Internet at http://pubs.acs.org.

References

(1) Karplus, M.; McCammon, J. A. *Nature Sturct. Biol.* **2002**, *9*, 646−652.

(2) Karplus, M. *Acc. Chem. Res.* **2002**, *35*, 321−323.

(3) *Computational Biochemistry and Biophysics*; Becker, O. M., MacKerell, A. D., Jr.; Roux, B., Watanabe, M., Eds.; Marcel-Dekker: New York, 2001; p 512.

(4) MacKerell, A. D., Jr. *J. Comput. Chem.* **2004**, *25*, 1584−1604.

(5) Beveridge, D. L.; McConnell, K. J. *Curr. Opin. Struct. Biol.* **2000**, *10*, 182−196.

(6) Auffinger, P.; Westhof, E. *Curr. Opin. Struct. Biol.* **1998**, *8*, 227−236.

(7) Cheatham, T. E., III. *Curr. Opin. Struct. Biol.* **2004**, *14*, 360−367.

(8) Norberg, J.; Nilsson, L. *Acc. Chem. Res.* **2002**, *35*, 465−472.

(9) Cheatham, T. E., III.; Young, M. A. *Biopolymers* **2000**, *56*, 232−256.

(10) Cheatham, T. E., III.; Kollman, P. A. *Annu. Rev. Phys. Chem.* **2000**, *51*, 435−471.

(11) Giudice, E.; Lavery, R. *Acc. Chem. Res.* **2002**, *35*, 350−357.

(12) MacKerell, A. D., Jr.; Nilsson, L. Nucleic Acid Simulations. In *Computational Biochemistry and Biophysics*; Becker, O. M., MacKerell, A. D., Jr., Roux, B., Watanabe, M., Eds.; Marcel Dekker: New York, 2001; pp 441−464.

(13) Foloppe, N.; MacKerell, A. D., Jr. *J. Comput. Chem.* **2000**, *21*, 86−104.

(14) MacKerell, A. D., Jr.; Banavali, N. K. *J. Comput. Chem.* **2000**, *21*, 105−120.

(15) Cheatham, T. E., III; Cieplak, P.; Kollman, P. A. *J. Biomol. Struct. Dyn.* **1999**, *16*, 845−861.

(16) Cornell, W. D.; Cieplak, P.; Bayly, C. I.; Gould, I. R.; Merz, K. M.; Ferguson, D. M.; Spellmeyer, D. C.; Fox, T.; Caldwell, J. W.; Kollman, P. A. *J. Am. Chem. Soc.* **1995**, *117*, 5179−5197.

(17) Langley, D. R. *J. Biomol. Struct. Dyn.* **1998**, *16*, 487−509.

(18) Feig, M.; Pettitt, B. M. *J. Phys. Chem. B* **1997**, *101*, 7361−7363.

(19) Feig, M.; Pettitt, B. M. *Biophys. J.* **1998**, *75*, 134−149.

(20) Cheatham, T. E., III.; Kollman, P. A. *J. Mol. Biol.* **1996**, *259*, 434−444.

(21) Reddy, S. Y.; LeClerc, F.; Karplus, M. *Biophy. J.* **2003**, *84*, 1421−1449.

(22) Cheng, X.; Roberts, R. J. *Nucleic Acids Res.* **2001**, *29*, 3784−3795.

(23) Hornby, D. P.; Ford, G. C. *Curr. Opin. Biotechnol.* **1998**, *9*, 354−358.

(24) Roberts, R. J. *Cell* **1995**, *82*, 9−12.

(25) Roberts, R. J.; Cheng, X. *Annu. Rev. Biochem.* **1998**, *67*, 181−198.

(26) Stivers, J. T. *Prog. Nucleic Acid Res. Mol. Biol.* **2004**, *77*, 37−65.

(27) Goedecke, K.; Pignot, M.; Goody, R. S.; Scheidig, A. J.; Weinhold, E. *Nature Struct. Biol.* **2001**, *8*, 101−103.

(28) Klimasauskas, S.; Kumar, S.; Roberts, R. J.; Cheng, X. *Cell* **1994**, *76*, 357−369.

(29) Cheng, X.; Blumenthal, R. M. *Structure* **1996**, *4*, 639−645.

(30) Lyakhov, I. G.; Hengen, P. N.; Rubens, D.; Schneider, T. D. *Nucleic Acids Res.* **2001**, *29*, 4892−4900.

(31) Varnai, P.; Canalia, M.; Leroy, J. L. *J. Am. Chem. Soc.* **2004**, *126*, 14659−14667.

(32) Dornberger, U.; Leijon, M.; Fritzsche, H. *J. Biol. Chem.* **1999**, *274*, 6957−6962.

(33) Gueron, M.; Leroy, J. L. *Methods Enzymol.* **1995**, *261*, 383−413.

(34) Chen, C. J.; Russu, I. M. *Biophys. J.* **2004**, *87*, 2545−2551.

(35) Moe, J. G.; Foltastogniew, E.; Russu, I. M. *Nucleic Acids Res.* **1995**, *23*, 1984−1989.

(36) Banavali, N. K.; MacKerell, A. D., Jr. *J. Mol. Biol.* **2002**, *319*, 141−160.

(37) MacKerell, A. D., Jr.; Brooks, B.; Brooks, C. L., III.; Nilsson, L.; Roux, B.; Won, Y.; Karplus, M. CHARMM: The Energy Function and Its Paramerization with an Overview of the Program. In *Encyclopedia of Computational Chemistry*; Schleyer, P. v. R., Allinger, N. L., Clark, T., Gasteiger, J., Kollman, P. A., Schaefer, H. F., III, Schreiner, P. R., Eds.; John Wiley & Sons: Chichester, 1998; Vol. 1, pp 271−277.

(38) Brooks, B. R.; Bruccoleri, R. E.; Olafson, B. D.; States, D. J.; Swaminathan, S.; Karplus, M. *J. Comput. Chem.* **1983**, *4*, 187−217.

(39) Quanta. 4.0 ed.; Accelrys Inc.: San Diego, CA, 2001.

(40) Field, M. J.; Karplus, M. CRYSTAL Module of CHARMM, 22nd ed.; Harvard University: Cambridge, MA, 1992.

(41) Darden, T.; York, D.; Pedersen, L. *J. Chem. Phys.* **1993**, *98*, 10089−10092.

(42) Steinbach, P. J.; Brooks, B. R. *J. Comput. Chem.* **1994**, *15*, 667−683.

(43) Ryckaert, J.-P.; Ciccotti, G.; Berendsen, H. J. C. *J. Comput. Phys.* **1977**, *23*, 327−341.

(44) Nosé, S. *J. Chem. Phys.* **1984**, *81*, 511−519.

(45) Beglov, D.; Roux, B. *J. Phys. Chem. B* **1997**, *101*, 7821−7826.

(46) Kumar, S.; Bouzida, D.; Swendsen, R. H.; Kollman, P. A.; Rosenberg, J. M. *J. Comput. Chem.* **1992**, *13*, 1011.

(47) Crouzy, S.; Baudry, J.; Smith, J. C.; Roux, B. *J. Comput. Chem.* **1999**, *20*, 1644−1658.

(48) Pan, Y. P.; Priyakumar, U. D.; MacKerell, A. D. *Biochemistry* **2005**, *44*, 1433−1443.

(49) Huang, N.; Banavali, N. K.; MacKerell, A. D., Jr. *Proc. Natl. Acad. Sci. U.S.A.* **2003**, *100*, 68−73.

(50) Giudice, E.; Várnai, P.; Lavery, R. *ChemPhysChem* **2001**, *11*, 673−677.

(51) Giudice, E.; Lavery, R. *J. Am. Chem. Soc.* **2003**, *125*, 4998−4999.

(52) Giudice, E.; Varnai, P.; Lavery, R. *Nucleic Acids Res.* **2003**, *31*, 2703−2703.

(53) Varnai, P.; Lavery, R. *J. Am. Chem. Soc.* **2002**, *124*, 7272−7273.

(54) Mol, C. D.; Izumi, T.; Mitra, S.; Tainer, J. *Nature* **2000**, *403*, 451−456.

(55) Wärmländer, S.; Sen, A.; Leijon, M. *Biochemistry* **2000**, *39*, 607−615.

(56) Warmlander, S.; Sandstrom, K.; Leijon, M.; Graslund, A. *Biochemistry* **2003**, *42*, 12589−12595.

(57) Guéron, M.; Kochoyan, M.; Leroy, J.-L. *Nature* **1987**, *328*, 89−92.

(58) Klimasauskas, S.; Szyperski, T.; Serva, S.; Wuthrich, K. *EMBO J.* **1998**, *17*, 317−324.

(59) Truhlar, D. G.; Garrett, B. C.; Klippenstein, S. J. *J. Phys. Chem.* **1996**, *100*, 12771−12800.

(60) Albery, W. J. *Adv. Phys. Org. Chem.* **1993**, *28*, 139−170.

(61) Lee, B.; Richards, F. M. *J. Mol. Biol.* **1971**, *55*, 379−400.

(62) Brameld, K.; Dasgupta, S.; Goddard, W. A., III. *J. Phys. Chem. B* **1997**, *101*, 4851−4859.

(63) Hobza, P.; Kabelac, M.; Sponer, J.; Mejzlik, P.; Vondrasek, J. *J. Comput. Chem.* **1997**, *18*, 1136−1150.

(64) Yanson, I. K.; Teplitsky, A. B.; Sukhodub, L. F. *Biopolymers* **1979**, *18*, 1149−1170.

(65) Cheng, Y. K.; Pettitt, B. M. *Prog. Biophys. Mol. Biol.* **1992**, *58*, 225−257.

(66) Sponer, J.; Leszczynski, J.; Hobza, P. *Biopolymers* **2001**, *61*, 3−31.

(67) Kool, E. T. *Annu. Rev. Biophys. Biomol. Struct.* **2001**, *30*, 1−22.

(68) Gago, F. *Methods-a Companion Methods Enzymol.* **1998**, *14*, 277−292.

(69) Hobza, P.; Sponer, J. *J. Am. Chem. Soc.* **2002**, *124*, 11802−11808.

(70) Hobza, P.; Sponer, J. *Chem. Rev.* **1999**, *99*, 3247−3276.

(71) Hobza, P.; Selzle, H. L.; Schlag, E. W. *J. Phys. Chem.* **1996**, *100*, 18790−18794.

(72) Hobza, P.; Selzle, H. L.; Schlag, E. W. *J. Am. Chem. Soc.* **1994**, *116*, 3500−3506.

(73) Saenger, W.; Hunter, W. N.; Kennard, O. *Nature* **1986**, *324*, 385−388.

CT0501957